β-$Bi_4(P_2Se_6)_3$: A New Ternary Selenophosphate Obtained in a P_2Se_5 Flux

Jennifer A. Aitken,[†] Shannon Brown,[†] Konstantinos Chondroudis,[†] Stéphane Jobic,[‡] Raymond Brec,[‡] and Mercouri G. Kanatzidis*,[†]

Department of Chemistry, Michigan State University, East Lansing, Michigan 48824, and Institut des Matériaux de Nantes, B.P. 32229, 44322 Nantes Cedex 03, France

Received February 17, 1999

Bi metal dissolves in excess molten phosphorus selenide at 500 °C to yield black, rodlike, air- and water-stable β-$Bi_4(P_2Se_6)_3$ crystals. The phase crystallizes in the triclinic space group $P\bar{1}$ (No. 2) with the room-temperature cell parameters $a = 12.2303(8)$ Å, $b = 6.7640(4)$ Å, $c = 17.866$ Å, $\alpha = 90.493(6)°$, $\beta = 94.133(6)°$, and $\gamma = 91.163(6)°$. The new structure is a complicated, three-dimensional framework built from $[Bi_4Se_{22}]$ ribbons connected to each other by sharing selenium atoms. The $[P_2Se_6]^{4-}$ ethane-like units are found inside and between the $[Bi_4Se_{22}]$ ribbons. The compound is a semiconductor with a band gap of 1.32 eV. It melts with decomposition at 512 °C, converting partially to Bi_2Se_3 and a P_xSe_y glassy material. Far-IR and Raman spectra show characteristic stretches for the $[P_2Se_6]^{4-}$ ligand and Bi−Se vibrations. The structural and chemical relationships of this compound with the α-form are discussed.

Introduction

On the basis of recent studies, it has become clear that the optimum experimental conditions for the synthesis of new ternary/quaternary chalcophosphate compounds are provided by the polychalcophosphate flux method.[1] The group 15 metals, and in particular Bi, display a very rich solid-state chemistry due in part to the presence of a lone $6s^2$ pair. The latter may adopt stereochemically significant configurations that distort the local coordination of Bi or remain spherically distributed around the metal to give a nearly perfect octahedral geometry. Thiophosphate compounds in group 15 remain few, but their structural diversity is rich and ranges from the one-dimensional $A_3M(PS_4)_2$ (A = K, Rb, Cs; M = Sb, Bi)[2] to the layered-type $ABiP_2S_7$ (A = K, Rb)[2] and $Cs_3Bi_2(PS_4)_2$[3] phases to the three-dimensional framework of $Na_{0.16}Bi_{1.28}P_2S_6$.[3] There are also glassy versions of some of these compounds which are currently under investigation.[4] The corresponding selenide chemistry, although not as well developed, has revealed two groups. The first one, KMP_2Se_6 (M = Sb, Bi),[5] features an elaborate two-dimensional structure while the second, $Cs_8M_4(P_2Se_6)_5$ (M = Sb, Bi), which also exhibits a two-dimensional structure, presents interdigitated layers that form tunnels and contain M−M interactions.[6] The only group 15 ternary chalcophosphates known are the MPS_4[7,8] and $M_4(P_2Se_6)_3$[9] (M = Sb, Bi) phases, which have been synthesized via direct combination reactions or vapor-transport techniques.

Our attempts to synthesize $BiPSe_4$ as an analogue of MPS_4 resulted in a new ternary compound which appears to be a second modification of $Bi_4(P_2Se_6)_3$.[9] The new compound, β-$Bi_4(P_2Se_6)_3$, adopts a new three-dimensional structure type, and herein we report on its synthesis, structural characterization, spectroscopic characterization, and thermal properties. Our work with this system and attempts to synthesize α-$Bi_4(P_2Se_6)_3$ resulted only in the β form reported here. Therefore, the nature of α-$Bi_4(P_2Se_6)_3$ and the origin of its chemical stability at this stage are somewhat uncertain.

Table 1. Crystallographic Data and Experimental Details for β-$Bi_4(P_2Se_6)_3$

empirical formula	$Bi_4P_6Se_{18}$
space group	$P\bar{1}$ (No. 2)
cell parameters	$a = 12.2303(8)$ Å
(from powder data at room temp)	$b = 6.7640(4)$ Å
	$c = 17.866(1)$ Å
	$\alpha = 90.493(6)°$
	$\beta = 94.133(6)°$
	$\gamma = 91.163(6)°$
	$V = 1473.8(2)$ Å^3
molecular wt	2443.04
density (calcd)	5.504 g·cm^{-3}
Z	2
linear abs coeff.	463.6 cm^{-1}
refinement results[a]	$R = 3.96\%$
	$R_w = 4.27\%$

[a] $R = \sum(|F_o| - |F_c|)/\sum|F_o|$. $R_w = [\sum w(|F_o| - |F_c|)^2/\sum w|F_o|^2]^{1/2}$.

Experimental Section

Reagents. Reagents in this work were used as obtained unless otherwise noted: (i) bismuth chunks, 99.999%, Noranda Advanced Materials, St. Laurent, Quebec, Canada; (ii) selenium shots, 99.999%, Noranda Advanced Materials, Quebec, Canada; (iii) red phosphorus powder, 100 mesh, EM Science, Gibbstown, NJ; (iv) *N*,*N*-dimethylformamide (DMF), 99.8%, ACS reagent grade, Aldrich Chemical Co., Inc., Milwaukee, WI; (v) diethyl ether, ACS grade, anhydrous, Columbus Chemical Industries, Inc., Columbus, WI; (vi) tri-*n*-bu-

[†] Michigan State University.
[‡] Institut des Matériaux.

(1) Kanatzidis, M. G. *Curr. Opinion Solid State Mater. Sci.* **1997**, *2*, 139.
(2) McCarthy, T. J.; Kanatzidis, M. G. *J. Alloys Comp.* **1996**, *236*, 70.
(3) McCarthy, T. J.; Kanatzidis, M. G. *Chem. Mater.* **1993**, *5*, 1061.
(4) Breshears, J. D.; Kanatzidis, M. G. Work in progress.
(5) McCarthy, T. J.; Kanatzidis, M. G. *J. Chem. Soc., Chem. Commun.* **1994**, 1089.
(6) McCarthy, T. J.; Hogan, T.; Kannewurf C. R.; Kanatzidis, M. G. *Chem. Mater.* **1994**, *6*, 1072.
(7) D'ordyai, V. S.; Galagovets, I. V.; Peresh, E. Y.; Voroshilov, Y. V.; Gerasimenko, V. S.; Slivka, V. Y. *Russ. J. Inorg. Chem. (Engl. Transl.)* **1979**, 24, 1603.
(8) Toffoli, P. P.; Khodadad, P.; Rodier, N. *Bull. Soc. Chim. Fr.* **1981**, *11−12*, 429.
(9) Ruck, M. *Z. Anorg. Allg. Chem.* **1985**, *621*, 1344.

10.1021/ic990180h CCC: $18.00
Published on Web 09/29/1999

Table 2. Fractional Atomic Coordinates and Equivalent Isotropic Atomic displacement parameters (Å^2) of β-$Bi_4(P_2Se_6)_3$

atom	*x*	*y*	*z*	U_{eq}[a]
Bi(1)	0.4656(1)	−0.9342(2)	0.8132(1)	0.0189(5)
Bi(2)	−0.1031(1)	−0.0218(3)	0.8850(1)	0.0273(6)
Bi(3)	0.0388(1)	−0.4288(3)	0.6893(1)	0.0222(5)
Bi(4)	0.6113(3)	−0.5265(6)	0.6189(3)	0.0408(7)
$Bi(4)_{max}$[b]	0.6049(3)	−0.5250(6)	0.6167(3)	
P(1)	0.2549(7)	0.554(1)	0.1787(6)	0.007(3)
P(2)	0.8269(7)	0.071(1)	0.1128(6)	0.009(3)
P(3)	0.4887(8)	0.059(1)	0.4427(6)	0.011(3)
P(4)	0.0793(7)	0.435(1)	0.4865(6)	0.011(3)
P(5)	0.4147(7)	0.432(2)	0.1500(6)	0.011(3)
P(6)	0.8365(7)	0.943(1)	0.2279(6)	0.009(3)
Se(1)	0.4905(3)	0.6474(6)	0.0779(2)	0.014(1)
Se(2)	0.5939(3)	0.3333(6)	0.4449(2)	0.013(1)
Se(3)	0.5108(3)	0.3799(5)	0.2571(2)	0.012(1)
Se(4)	0.3783(3)	0.1591(6)	0.0844(2)	0.013(1)
Se(5)	0.1921(3)	0.3135(6)	0.2464(2)	0.016(1)
Se(6)	0.1659(3)	0.6070(6)	0.0709(2)	0.018(1)
Se(7)	0.0141(3)	0.8869(6)	0.2523(2)	0.014(1)
Se(8)	0.8302(3)	0.6371(6)	0.4073(2)	0.017(1)
Se(9)	0.2972(3)	0.8143(6)	0.2492(2)	0.014(1)
Se(10)	0.6562(3)	0.1448(6)	0.0831(2)	0.015(1)
Se(11)	0.1484(3)	0.6575(6)	0.4145(3)	0.018(1)
Se(12)	0.9409(3)	0.3272(5)	0.1150(2)	0.014(1)
Se(13)	0.5618(3)	0.8358(6)	0.3729(2)	0.015(1)
Se(14)	0.7721(3)	0.1644(6)	0.3013(2)	0.017(1)
Se(15)	0.7342(3)	0.6795(6)	0.2199(2)	0.017(1)
Se(16)	0.3167(3)	0.1180(6)	0.4192(2)	0.017(1)
Se(17)	0.8960(3)	0.8308(6)	0.0480(2)	0.015(1)
Se(18)	0.0305(3)	0.1680(6)	0.4207(2)	0.018(1)

[a] $U_{eq}=(\sum_i\sum_j U_{ij}a_i^*a_j^*a_i\cdot a_j)/3$. [b] $Bi(4)_{max}$ corresponds to the maximum of the probability density function of Bi(4).

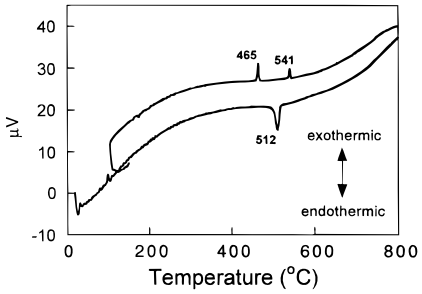

Figure 1. DTA diagram of β-$Bi_4(P_2Se_6)_3$. The decomposition of β-$Bi_4(P_2Se_6)_3$ is indicated by the endothermic peak. The two exothemic peaks at 541 and 465 °C correspond to the crystallization of Bi_2Se_3 and recrystallization of β-$Bi_4(P_2Se_6)_3$, respectively. Heating rate: 10 °C/min.

tylphosphine, tech, Lancaster Synthesis Inc., Windham, NH; (vii) ethylenediamine, J. T. Baker, Phillipsburg, NJ. The chunks and shots were ground to fine powders before being used.

Synthesis of P_2Se_5. P_2Se_5 was prepared by heating a stoichiometric ratio of the elements in an evacuated Pyrex ampule. The mixture was heated to 460 °C in 30 h and kept at 460 °C for 24 h. It was then cooled to 50 °C in 10 h. The P_2Se_5 was ground and stored in a nitrogen glovebox.

Synthesis of β-$Bi_4(P_2Se_6)_3$. Method I (Initial Synthesis). Single crystals of β-$Bi_4(P_2Se_6)_3$ were obtained from a mixture of 0.209 g of Bi (1 mmol), 0.372 g of P (12 mmol), and 3.948 g of Se (50 mmol), which was heated in an evacuated Pyrex tube to 500 °C. The temperature remained at 500 °C for 3 days, followed by cooling to 50 °C at 3 °C/h. The product was first washed with DMF for 2 days and dried with anhydrous ether. To remove residual flux, the product was then washed with tri-*n*-butylphosphine for about 1 h. Further washing with ether gave 60% black, irregular rodlike, air- and water-stable crystals of β-$Bi_4(P_2Se_6)_3$ and 40% silver plates of Bi_2Se_3. Semiquantitative microprobe analysis of the rodlike crystals gave a composition of $Bi_4P_{6.2}Se_{18.3}$. The powder diffraction pattern of the rodlike crystals

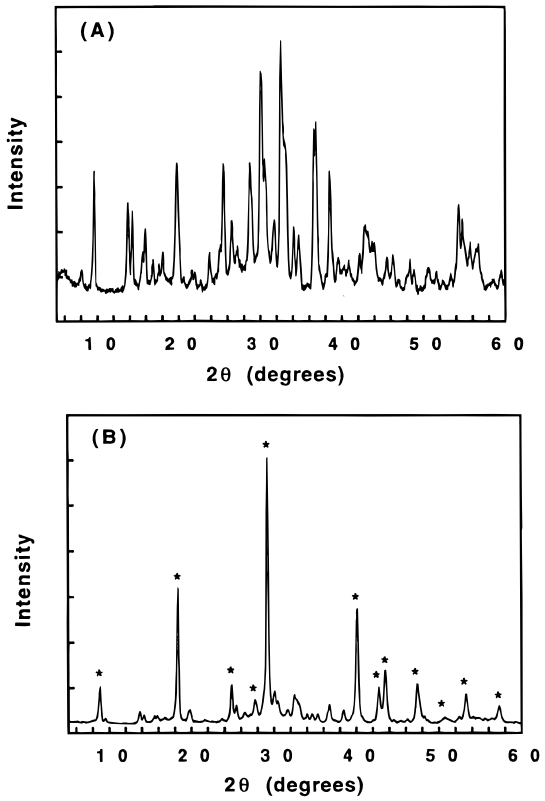

Figure 2. Powder X-ray diffraction patterns of (A) a pure-phase sample of β-$Bi_4(P_2Se_6)_3$ before DTA and (B) the sample after DTA, which shows the partial decomposition of β-$Bi_4(P_2Se_6)_3$ to Bi_2Se_3 and P_xSe_y. In part B, the stars indicate the peaks which can be indexed to Bi_2Se_3, the unlabeled peaks correspond to β-$Bi_4(P_2Se_6)_3$, and there are no peaks observed for the P_xSe_y material because it is X-ray amorphous.

indicated a new phase, while the powder diffraction pattern of the plates was indexed to Bi_2Se_3.

Method II. β-$Bi_4(P_2Se_6)_3$ was also prepared by a direct stoichiometric reaction from a mixture of 0.836 g of Bi (4 mmol), 0.186 g of P (6 mmol), and 1.421 g of Se (18 mmol). The mixture was heated in an evacuated quartz tube to 600 or 760 °C for 2 days, followed by cooling to 50 °C at 8 °C/h, giving 50% black, irregular rodlike, air- and water-stable crystals of β-$Bi_4(P_2Se_6)_3$ and 50% silver plates of Bi_2Se_3.

Method III (Optimum Synthesis). A 0.209 g (1 mmol) sample of Bi and 1.827 g (4 mmol) of P_2Se_5 were thoroughly mixed and transferred to a Pyrex tube, which was flame-sealed under vacuum. The reaction mixture was heated to 500 °C over a 24 h period. This temperature was maintained for 3 days and then decreased to 280 °C at a rate of 3 °C/h and to 50 °C in 2 h. The product was washed with a solution of 3 parts of DMF and 1 part of ethylenediamine under an atmosphere of nitrogen to dissolve the excess P_xSe_y flux. The solution was decanted, and the product was washed with anhydrous ether, giving 100% pure β-$Bi_4(P_2Se_6)_3$ as black rodlike crystals and a black powder (80/20%). The powder diffraction pattern showed no evidence of Bi_2Se_3.

Physical Measurements. Electron Microscopy. Semiquantitative microprobe analysis of the compound was performed with a JEOL JSM-35C scanning electron microscope (SEM) equipped with a Tracor Northern energy dispersive spectroscopy (EDS) detector. Data were acquired with an accelerating voltage of 20 kV and a 40 s accumulation time.

Differential Thermal Analysis. Differential thermal analysis (DTA) was performed with a computer-controlled Shimadzu DTA-50 thermal analyzer. Approximately 15 mg of the sample was sealed in a carbon-coated quartz ampule under vacuum. A quartz ampule containing alumina of equal mass was sealed and placed on the reference side of the detector. The sample was heated to 800 °C at 10 °C/min, isothermed for 5 min, and then cooled at a rate of 10 °C/min to 100 °C, followed by rapid cooling to room temperature. Residues of the DTA experiment

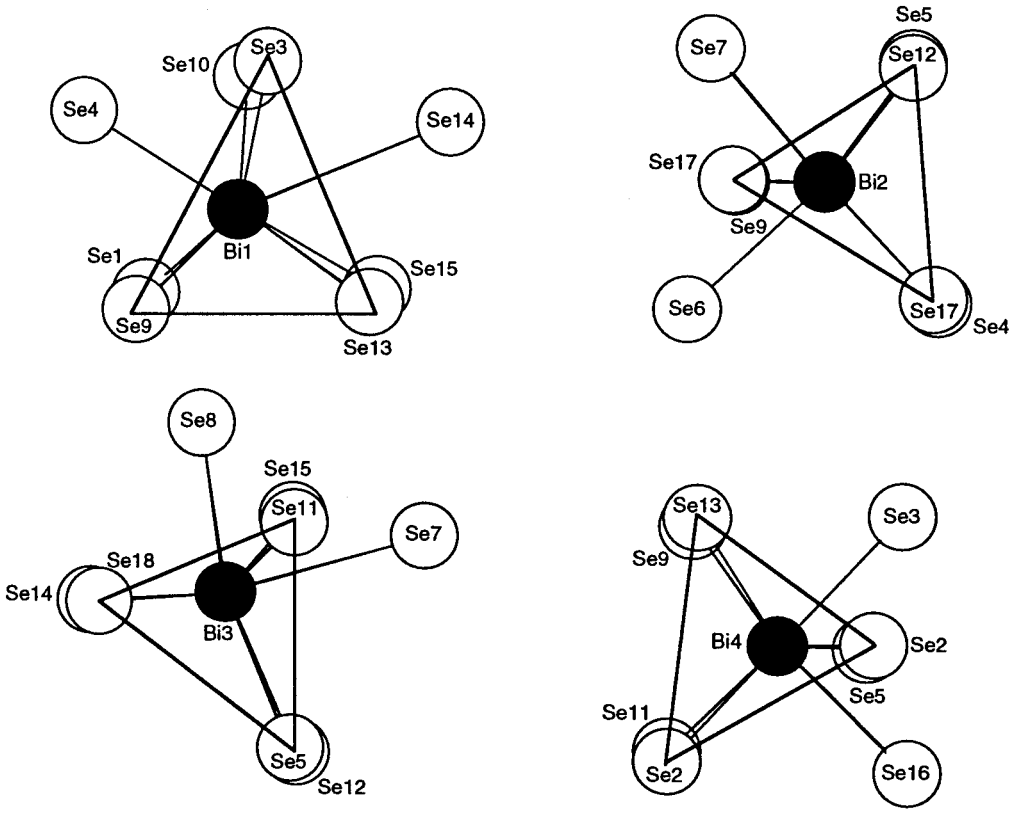

Figure 3. Immediate coordination spheres of the bismuth atoms in β-$Bi_4(P_2Se_6)_3$. The best description is the one of bicapped trigonal prisms. The triangles are drawn to guide the eye to the trigonal prismatic face and help identify the two capping atoms.

were examined by powder X-ray diffraction. To evaluate congruent melting, we compared the powder X-ray diffraction patterns before and after the DTA experiments. The stability and reproducibility of the samples were monitored by running multiple heating and cooling cycles.

Solid-State UV/Vis/Near-IR Spectroscopy. An optical diffuse reflectance measurement was performed at room temperature using a Shimadzu UV-3101PC double-beam, double-monochromator spectrophotometer. The instrument was equipped with an integrating sphere and controlled by a personal computer. $BaSO_4$ was used as a 100% reflectance standard. The sample was prepared by grinding the crystals to a powder and spreading it on a compacted surface of the powdered standard material, preloaded into a sample holder. The reflectance versus wavelength data generated were used to estimate the material's band gap by converting reflectance to absorption data.[10]

Infrared Spectroscopy. The FT-IR spectrum was recorded for a solid in a CsI matrix. The sample was ground with dry CsI into a fine powder and pressed into translucent pellets. The spectrum was recorded in the far-IR region (600−100 cm^{-1}, 4 cm^{-1} resolution) with the use of a Nicolet 740 FT-IR spectrometer equipped with a TGS/PE detector and silicon beam splitter.

Raman Spectroscopy. The Raman spectrum was recorded on a Holoprobe Raman spectrograph equipped with a 633 nm HeNe laser and a CCD camera detector. The instrument was coupled to an Olympus BX60 microscope. Crystals were simply placed onto a small glass slide, and a 50× objective lens was used to choose the area of the crystal specimens to be measured. The spot size of the laser beam was 10 μm when the 50× objective lens was used.

Single-Crystal X-ray Crystallography. A tiny, well-shaped single crystal (0.10 × 0.015 × 0.015 mm) was chosen and placed on the outside of a split silica capillary under an inert atmosphere. Large crystals, selected to obtain a larger diffracting volume and to allow the measurements of the sample faces for absorption corrections, yielded multiple diffraction peaks, indicative of fairly systematic twinning. The initial tiny, visually almost unobservable single crystal was thus kept for data collection. The crystal diffraction recording was carried out on a STOE Image Plate X-ray diffractometer (Mo Kα radiation and graphite monochromator) at room temperature. First, a series of 10 diffraction patterns was recorded by rotating the unoriented crystal in the X-ray beam. The crystal lattice and the cell parameter determination were then achieved from the analysis of 260 reflections. Indexing was performed using the program INDEX.[11] Images were then collected over a 250° ϕ range with a 1.0° increment angle and a 5 min exposure time per reflection. A reindexing procedure over the 250 images and unsuccessful attempts in increasing the lattice symmetry asserted the triclinic cell without any ambiguity. More accurate cell parameters were then determined from a least-squares refinement of the setting angles of 1352 reflections in the $3.8° \le 2\theta \le 56.3°$ range, yielding $a = 12.199(2)$ Å, $b = 6.7692(9)$ Å, $c = 17.859(3)$ Å, $\alpha = 90.21(2)°$, $\beta = 94.19(2)°$, and $\gamma = 91.02(1)°$.

Reflections were recorded in the $-16 \le h \le 16$, $-8 \le k \le 8$, $-23 \le l \le 23$ space. After the Lorentz−polarization reduction of the 17396 raw data, a set of 4305 reflections with $I \ge 3\sigma(I)$ was obtained. The structure was solved in the $P\bar{1}$ space group (2222 independent reflections) from a Patterson analysis followed by successive observed and difference Fourier syntheses calculated with the JANA98[12] structure determination package. An attempt to refine the structure in the $P1$ space group failed. Conventional atomic and anomalous scattering factors were taken from the usual sources. A weighting scheme based on $\sigma(F_o)$ corrected with an instability coefficient was used.

The first refinement cycle series with isotropic atomic displacement parameters (ADPs) (113 variables) yielded an R value of 6.92%. The introduction of anisotropic ADPs for all the atomic positions (253 variables) led to $R_F = 4.50\%$ and $R_{wF} = 4.74\%$ with a high isotropic ADP for Bi(4) (U_{eq}(Bi(4)) = 0.0399(7) Å^2) compared to those of the

(10) (a) Wendlandt, W. W.; Hecht, H. G. *Reflectance Spectroscopy*; Interscience Publishers: New York, 1966. (b) Kotüm, G. *Reflectance Spectroscopy*; Springer-Verlag: New York, 1969. (c) Tandon, S. P.; Gupta, J. P. *Phys. Status Solidi* **1970**, *38*, 363−367.

(11) *STOE SPOS Software Manual*, version 2.75; STOE & CIE GmbH: Darmstadt, Germany, 1996.

(12) Petricek, V.; Dusek, M. JANA98, *Crystallographic Computing System*; Institute of Physics, Academy of Sciences of the Czech Republic; Prague, 1998.

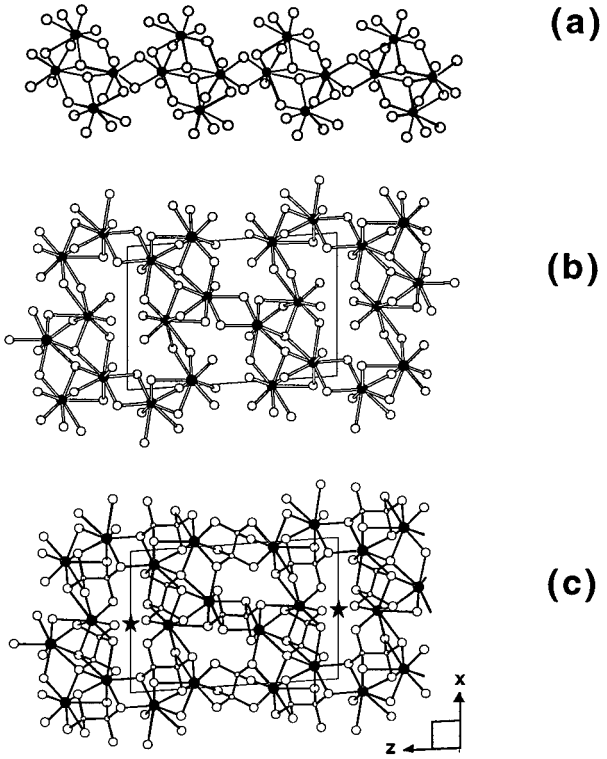

Figure 4. Structure description of β-$Bi_4(P_2Se_6)_3$: (a) infinite $[Bi_4Se_{22}]$ ribbon running along *b*; (b) assembly of the $[Bi_4Se_{22}]$ ribbons through selenium edge sharing, defining two-dimensional planes parallel to the *ab* plane; (c) view along the *b* axis of the β-$Bi_4(P_2Se_6)_3$ structure showing the bonding due to the P_2 pairs engaged in $[P_2Se_6]$ units. Key: black circles, Bi; large open circles, Se, small open circles, P.

other bismuth atoms (mean $U_{eq} = 0.0227(6)$ Å^2) and significant electron density residues ranging from -3.40 to $+3.90$ e/Å^3 with maxima around Bi(4). This motivated a nonharmonic refinement of the Bi(4) ADP to better describe the electronic density around this site, and a Gram−Charlier expansion[13] of the atomic displacement factor at the third order was introduced. The R_F and R_{wF} dropped meaningfully to 3.96% and 4.27%, respectively, while the electron density residues ranged from -2.17 to $+2.57$ e/Å^3. No significant electron density was then found in the difference Fourier map in the vicinity of the Bi(4) site. The nonharmonic refinement all owed the mean Bi(4) atomic position to be distinguished from the position of the Bi(4) nonharmonic probability density function maximum. These two sites are separated by 0.086(4) Å. Attempts to refine the structure with a split model led to high correlations, and thus the model was not considered as acceptable for the structure description. The refinement results for this final nonharmonic model including third-order tensor elements of Bi(4) atomic displacement parameters are deposited with the Supporting Information. To explain the origin of the Bi(4) atom behavior, a temperature analysis of the bismuth distribution should be undertaken. Such an analysis should be carried out up to high diffraction angles on a four-circle diffractometer to better fit the thermal parameters. However, owing to the low symmetry of the crystal and its small diffracting power, such an experiment was not undertaken. See Table 1 for a summary of the crystallographic data and Table 2 for atomic positional and isotropic thermal parameters. Anisotropic temperature factors and structure factors are also deposited with the Supporting Information (CIF file).

Powder X-ray Diffraction. Powder diffraction diagrams were recorded in a Debye−Scherrer geometry (0.1 mm diameter Lindeman capillary) on an INEL CPS 120 X-ray powder diffractometer using monochromatized Cu Kα radiation ($\lambda = 1.540598$ Å) and equipped with a position-sensitive detector with a 2θ range of 0−120° calibrated with $Na_2Ca_3Al_{12}F_{14}$ as the standard.[14] Once the triclinic cell parameters were determined from the single-crystal analysis (see above), the reflections in the diagram could be entirely assigned to (*hkl*) planes with the FULLPROF powder refinement package. This gave the cell parameters $a = 12.2303(4)$ Å, $b = 6.7640(4)$ Å, $c = 17.866(1)$ Å, $\alpha = 90.493(6)°$, $\beta = 94.133(6)°$, $\gamma = 91.163(6)°$, and $V = 1473.8(2)$ Å^3. Neither the monoclinic form of $Bi_4(P_2Se_6)_3$ (cell volume 1495.6(3) Å^3) nor impurities were observed in our sample. The main d_{hkl} spacings (1−50° 2θ range) with observed intensities for β-$Bi_4(P_2Se_6)_3$ are deposited with the Supporting Information. The diagram was found to be totally different from the one calculated using the monoclinic cell parameters of α-$Bi_4(P_2Se_6)_3$.[9]

Results and Discussion

Synthesis and Thermal Analysis. β-$Bi_4(P_2Se_6)_3$ was initially obtained in 60% yield from the reaction of Bi/P/Se in a 1/12/50 molar ratio heated to 500 °C. Direct combination of the elements at 600 or 760 °C produced β-$Bi_4(P_2Se_6)_3$ and Bi_2Se_3 in about a 50%/50% ratio. Also, a direct combination reaction with 4 extra equiv of selenium gave the same result. The reaction of bismuth with 2 equiv of P_2Se_5 heated to 500 °C also resulted in a mixture of β-$Bi_4(P_2Se_6)_3$ and Bi_2Se_3. The best method to prepare single-phase β-$Bi_4(P_2Se_6)_3$ is in a P_2Se_5 flux according to eq 1, where the excess of P_2Se_5 is at least 4 equiv. It is very

$$\mathrm{Bi} + \mathrm{P_2Se_5(excess)} \xrightarrow{500\ °C} \beta\text{-}\mathrm{Bi_4(P_2Se_6)_3} + \mathrm{P_xSe_y} \quad (1)$$

puzzling that, in all of our synthetic experiments, we never produced any of the α-$Bi_4(P_2Se_6)_3$ compound, even though we have been able to reproduce the synthesis of isostructural $Sb_4(P_2Se_6)_3$, which appeared in the same publication.[9]

β-$Bi_4(P_2Se_6)_3$ seems to be relatively air stable for at least several months. The thermal stability is not very high, as seen in the DTA diagram shown in Figure 1. The compound does not melt congruently; it precipitates out Bi_2Se_3 and a P_xSe_y glassy material. There is an endothermic peak in the DTA diagram at 512 °C corresponding to a melting point. On cooling from 800 °C, Bi_2Se_3 crystallizes from the melt at 541 °C, and then at 465 °C, β-$Bi_4P_2Se_6$ recrystallizes using the remaining bismuth. The excess phosphorus and selenium in the tube form a glassy material. Two additional heating−cooling cycles did not alter the positions of the peaks or their relative intensity. These observations are confirmed by visual inspection and powder X-ray diffraction. The product after the DTA experiment contained three different products: (1) a small amount of black, rodlike crystals of β-$Bi_4(P_2Se_6)_3$, (2) a greater amount of silver colored, platelike crystals of Bi_2Se_3, and (3) a red glassy material of P_xSe_y. Powder X-ray diffraction confirmed the presence of β-$Bi_4(P_2Se_6)_3$ and Bi_2Se_3. The P_xSe_y residue does not appear in the diffraction pattern because it is amorphous. The powder X-ray diffraction patterns before and after DTA are shown in Figure 2. We were surprised by the lack of α-$Bi_4(P_2Se_6)_3$ and again questioned the stability of this compound. The α phase, which is said to be prepared via high-temperature synthesis,[9] should be more thermodynamically favorable than the β phase, and one would expect that, upon heating, the β phase may transform to the α phase. This is clearly not what we observed.

Structure Description. The structure of β-$Bi_4(P_2Se_6)_3$ is a complex three-dimensional ensemble whose skeleton is based on the stacking of face- and edge-sharing eight-coordinated Bi polyhedra. The best description of these polyhedra is that of a bicapped trigonal prism, although the prism is somewhat

(13) Wilson, A. J. C. *International Tables for X-ray Crystallography*, 3rd revised edition; Kluwer Academic Publishers: Boston, 1995; Vol. C, p 507.

(14) Evain, M.; Deniard, P.; Jouanneaux, A.; Brec, R. *J. Appl. Crystallogr.* **1993**, *26*, 563−569,

Table 3. Bond Distances (Å) and Angles (deg) in β-$Bi_4(P_2Se_6)_3$ Polyhedra

		Bi(1) Environment	
Bi(1)−Se(1)	2.752(4)	Bi(1)−Se(14)	3.737(4)
Bi(1)−Se(3)	3.282(4)	Bi(1)−Se(15)	3.045(4)
Bi(1)−Se(4)	2.994(4)	Bi(1)−P(5)	3.742(9)
Bi(1)−Se(9)	3.271(4)	Bi(1)−P(5)	3.706(9)
Bi(1)−Se(10)	2.835(4)	Bi(1)−P(6)	3.714(9)
Bi(1)−Se(13)	3.390(4)		
		Bi(2) Environment	
Bi(2)−Se(4)	3.556(4)	Bi(2)−Se(12)	2.893(4)
Bi(2)−Se(5)	3.171(4)	Bi(2)−Se(17)	3.088(5)
Bi(2)−Se(6)	3.037(4)	Bi(2)−Se(17)	2.987(4)
Bi(2)−Se(7)	2.900(5)	Bi(2)−P(2)	3.398(9)
Bi(2)−Se(9)	3.567(4)		
		Bi(3) Environment	
Bi(3)−Se(5)	3.232(4)	Bi(3)−Se(14)	2.888(4)
Bi(3)−Se(7)	3.344(4)	Bi(3)−Se(15)	3.579(4)
Bi(3)−Se(8)	2.826(4)	Bi(3)−Se(18)	2.752(5)
Bi(3)−Se(11)	3.205(4)	Bi(3)−P(4)	3.360(9)
Bi(3)−Se(12)	3.549(5)	Bi(3)−P(6)	3.832(9)
		Bi(4) Environment	
Bi(4)−Se(2)	3.234(6) [3.201(4)]	Bi(4)−Se(11)	3.182(6) [3.249(4)]
Bi(4)−Se(2)	3.009(5) [2.928(4)]	Bi(4)−Se(13)	2.959(6) [2.915(4)]
Bi(4)−Se(3)	2.936(6) [2.921(4)]	Bi(4)−Se(16)	2.982(6) [2.987(4)]
Bi(4)−Se(5)	3.551(6) [6.621(4)]	Bi(4)−P(3)	3.569(9) [3.523(9)]
Bi(4)−Se(9)	3.222(6) [3.281(4)]		
		P(1)P(5) Ethane−like Environment	
P(1)−Se(5)	2.195(9)	P(5)−Se(3)	2.205(9)
P(1)−Se(6)	2.178(9)	P(5)−Se(4)	2.199(9)
P(1)−Se(9)	2.188(9)	P(1)−P(5)	2.23(1)
P(5)−Se(1)	2.189(9)		
Se(5)−P(1)−Se(6)	116.8(4)	Se(1)−P(5)−Se(3)	114.0(4)
Se(5)−P(1)−Se(9)	110.3(5)	Se(1)−P(5)−Se(4)	108.3(5)
Se(5)−P(1)−P(5)	100.9(5)	Se(1)−P(5)−P(1)	107.1(5)
Se(6)−P(1)−Se(9)	116.5(5)	Se(3)−P(5)−Se(4)	112.9(5)
Se(5)−P(1)−P(5)	104.9(5)	Se(3)−P(5)−P(1)	106.9(5)
Se(9)−P(1)−P(5)	105.3(4)	Se(4)−P(5)−P(1)	107.2(5)
		P(2)P(6) Ethane−like Environment	
P(2)−Se(10)	2.186(9)	P(6)−Se(14)	2.176(9)
P(2)−Se(12)	2.199(9)	P(6)−Se(15)	2.157(9)
P(2)−Se(17)	2.205(9)	P(2)−P(6)	2.23(1)
P(6)−Se(7)	2.227(9)		
Se(10)−P(2)−Se(12)	113.8(5)	Se(7)−P(6)−Se(14)	113.9(4)
Se(10)−P(2)−Se(17)	116.9(5)	Se(7)−P(6)−P(15)	114.1(5)
Se(10)−P(2)−P(6)	107.9(4)	Se(7)−P(6)−P(2)	104.0(5)
Se(12)−P(2)−Se(17)	108.5(4)	Se(14)−P(6)−Se(15)	111.7(4)
Se(12)−P(2)−P(6)	107.5(5)	Se(14)−P(6)−P(2)	106.5(5)
Se(17)−P(2)−P(6)	101.2(5)	Se(15)−P(6)−P(2)	105.7(5)
		P(3)P(3) Ethane−like Environment	
P(3)−Se(2)	2.236(9)	P(3)−Se(16)	2.162(9)
P(3)−Se(13)	2.193(9)	P(3)−P(3)	2.21(1)
Se(2)−P(3)−Se(13)	108.6(4)	Se(13)−P(3)−Se(16)	117.6(5)
Se(2)−P(3)−Se(16)	112.6(5)	Se(13)−P(3)−P(3)	104.1(5)
Se(1)−P(3)−P(1)	104.7(5)	Se(16)−P(3)−P(3)	108.2(5)
		P(4)P(4) Ethane−like Environment	
P(4)−Se(8)	2.190(9)	P(4)−Se(18)	2.196(9)
P(4)−Se(11)	2.183(9)	P(4)−P(4)	2.23(1)
Se(8)−P(4)−Se(11)	118.8(4)	Se(11)−P(4)−Se(18)	110.1(5)
Se(8)−P(4)−Se(18)	111.6(5)	Se(11)−P(4)−P(4)	103.2(5)
Se(8)−P(4)−P(4)	107.7(5)	Se(18)−P(4)−P(4)	104.0(5)

distorted (see Figure 3). Four [$BiSe_8$] units are linked together through three selenium edges and two selenium triangular faces to form [Bi_4Se_{22}] ribbons propagating along the *b* axis (see Figure 4a). These ribbons are then linked to each other through edge-sharing along the *a* axis (see Figure 4b) to form two-dimensional [Bi_4Se_{20}] planes parallel to the *ab* face. These planes are in turn linked to each other along *c* via another sharing of Se−Se edges (see Figure 4b), a three-dimensional [Bi_4Se_{18}]

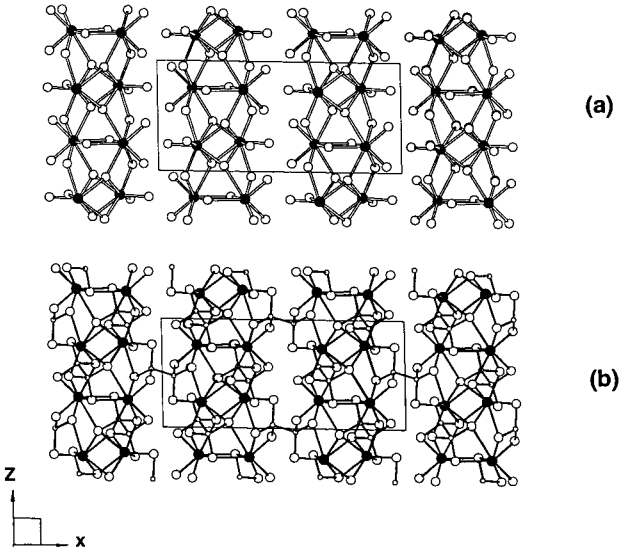

Figure 5. Structure of α-$Bi_4(P_2Se_6)_3$ (adapted from ref 9): (a) infinite $[Bi_4Se_{18}]$ layers running along the *bc* plane; (b) view along the *b* axis of the α-$Bi_4(P_2Se_6)_3$ structure showing the interlayer bonding through the phosphorus pairs. Atom identifications are the same as those of Figure 4.

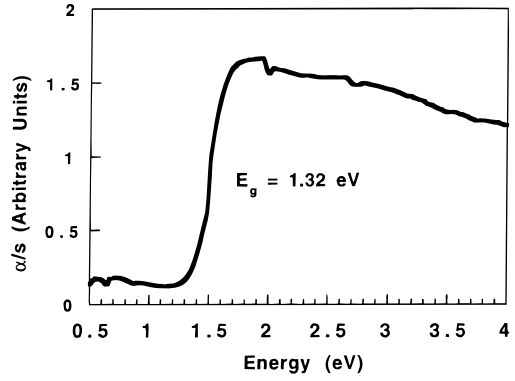

Figure 6. Optical absorption spectrum of β-$Bi_4(P_2Se_6)_3$.

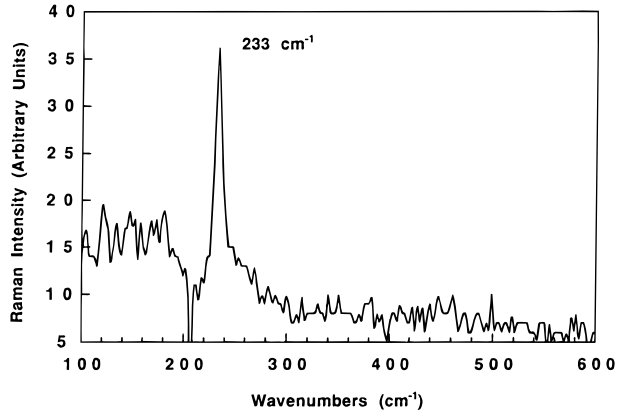

Figure 7. Raman spectrum of β-$Bi_4(P_2Se_6)_3$.

network being then obtained. This Bi−Se framework is a rather open structure with empty tunnels running along the *a* and *b* axes (see Figure 4b). The framework is then further linked through addition of phosphorus pairs that form $[P_2Se_6]^{4-}$ ethane-like units (see Figure 4c). It is worth underlining the fact that only half of the octahedral cavities contained in the *ab* planes are occupied by P−P pairs (see stars at the center of the empty sites in Figure 4c). In addition, according to their location along *b*, the selenophosphate $[P_2Se_6]^{4-}$ groups are oriented in two different directions approximately along the [0,−1,1] and [−5,4,1] axes.

The Bi−Se and P−Se distances in β-$Bi_4(P_2Se_6)_3$ are found in the 2.752(4) Å−3.737(4) and 2.157(9)−2.227(9) Å ranges, respectively. The P−P average bonding distance is 2.23(1) Å. All these distances agree well with those reported for α-$Bi_4(P_2Se_6)_3$. Moreover, the differences between the two allotropic forms do not lie in the first-neighbor coordination of Bi and P but in the three-dimensional arrangement of their polyhedra. In α-$Bi_4(P_2Se_6)_3$, and in contrast to β-$Bi_4(P_2Se_6)_3$, the corner-, edge- and square-face-sharing $[BiSe_8]$ entities define $[Bi_4Se_{18}]$ layers not interconnected via selenium ions along *a*, (see Figure 5a). Two-thirds of the P−P dimers are embedded within these layers shown in Figure 5b, while the remaining third connects together the Bi slabs, but this time on each side of the $[Bi_4Se_{18}]$ layers. Selected bond distances and angles are given in Table 3.

Spectroscopy. Solid-state UV/vis diffuse reflectance spectroscopy performed on β-$Bi_4(P_2Se_6)_3$ shows a sharp optical absorption consistent with semiconducting behavior. The energy band gap E_g, associated with this absorption edge, is ca. 1.32 eV (see Figure 6.)

The infrared spectrum displays absorptions at ca. 479 (w), 456 (vs), 446 (vs), 428 (vs), 288 (s), and 175 (s) cm^{-1}, consistent with the presence of the $[P_2Se_6]^{4-}$ ligand.[15] The absorption at ca. 175 cm^{-1} may be due to Bi−Se vibrations. The Raman spectrum, shown in Figure 7, exhibits a single peak at 233 cm^{-1}, which can be tentatively assigned to P−Se stretching vibrations.

Conclusion

The low-temperature flux method allowed the synthesis of a new allotropic form of $Bi_4(P_2Se_6)_3$. The differences between the α and the β forms are not due to changes in the coordination of selenium around bismuth and phosphorus; they are attributed to changes in the interconnection of the $[BiSe_8]$ and $[P_2Se_6]^{4-}$ constituting groups. β-$Bi_4(P_2Se_6)_3$ does not melt congruently; however, it does not convert to the α phase. β-$Bi_4(P_2Se_6)_3$ partially decomposes to Bi_2Se_3 and an amorphous P_xSe_y material when heated above 512 °C. In our hands, the reported synthesis technique for α-$Bi_4(P_2Se_6)_3$ does not yield the compound; instead, it gives only a mixture of β-$Bi_4(P_2Se_6)_3$ and Bi_2Se_3. A parallel synthesis of the antimony derivative did lead to the reported monoclinic $Sb_4(P_2Se_6)_3$[9] with the same structure as the supposed α-$Bi_4(P_2Se_6)_3$ phase. It is therefore puzzling why the α-$Bi_4(P_2Se_6)_3$ compound is not accessible. One possibility is that the α form is impurity stabilized.

Acknowledgment. Financial support from the National Science Foundation (Grant DMR-9817287) is gratefully acknowledged. This work made use of the SEM facilities of the Center for Electron Optics at Michigan State University. We acknowledge the use of the W. M. Keck Microfabrication Facility at Michigan State University, an NSF MRSEC facility. M.G.K. is an A. P. Sloan Foundation and a Camille and Henry Dreyfus Teacher-Scholar, 1993−1998.

Supporting Information Available: An X-ray crystallographic file in CIF format. This material is available free of charge via the Internet at http://pubs.acs.org.

IC990180H

(15) McCarthy, T. J.; Kanatzidis, M. G. *Inorg. Chem.* **1995**, *34*, 1257.